Influence of vibrations on indentation and compression strength of sea ice

**A. Marchenko[1], E. Karulin[2], R. Frederking[3], D. Cole[4], J. Brown[5], M. Karulina[2],
A. Sakharov[6], P. Chistyakov[6], D. Sodhi[4], V. Markov[6], B. Lishman[7],
M. Shortt[8], A. Sliusarenko[9]**

[1]*The University Centre in Svalbard*
PO Box 156, N-9171 Longyeabryen, Norway
Aleksey.Marchenko@unis.no
[2]*Krylov State Research Centre, St.-Petersburg, Russia*
[3]*National Research Council Canada, Ottawa, Canada*
[4]*Dartmouth College, Hannover, USA*
[5]*National Research Council Canada, St'-Johns, Canada*
[6]*Lomonosov Moscow State University, Moscow, Russia*
[7]*London South Bank University, London, UK*
[8]*University College London, London, UK*
[9]*Soft Engineering, Kiev, Ukrain*

Indentation and compression strengths of floating sea ice subjected to vibrations is discussed. The experiments were performed on the land fast ice of the Van-Mijen Fjord in March of 2018 and 2019. The ice thickness was around 70 cm, and the ice salinity was 4-5 ppt. Vibrations were introduced in the ice by the vibration plate with weight of 400 kg before the tests during 10-15 min. The vibration plate was standing and vibrating on the ice surface. The spectrum of vibrations was recorded with accelerometers. Analysis of thin sections of ice was performed on the place of the field works. Indentation tests were performed with the original hydraulic rig on natural ice and ice subjected to the action of vibrating plate. It was discovered that stroke rates tests were higher in the tests performed on the ice subjected to vibrations. Uniaxial compression tests were also performed on ice cores taken from the natural ice and from the ice subjected to the vibrations. Uniaxial compression strength of ice cores taken from the ice subjected to vibrations was higher than in the tests with natural ice.

1. Introduction

Vibrations can penetrate and influence ice properties due to the motions of aicrafts on ice runways, motions of cars or trains by ice roads, work of drilling rigs mounted on floating ice etc. A large group of inventions deal with vibration devices mounted on vessels or ice near vessels. It could be rotating unbalanced masses or power cylinders with a freely moving mass (Bogorodsky et al., 1987). An icebreaker attachment with a vibratory system has been developed and patented in few countries (Lezin, 1977).

Vibrations can influence ice properties in the vicinity of offshore structures due to the interaction of ice and structures. Frequency lock-in effect influence resonance interaction between structure and ice at natural frequencies of the structure (ISOPE 19906). Vibrations penetrate into the ice and potentially can change ice properties near the structure. For example, vibrations can influence micro-cracking of ice, make ice more "viscous" and influence synchronization of ice failure events along the contact surface with the structure.

In this paper we present results of field experiments performed on sea ice in 2018 and 2019. Vibrations were introduced in the ice by the vibrating plate (VP) designed for road works. Full scale indentation tests and uniaxial compression tests of ice cores were performed on natural sea ice and on sea ice subjected by VP action. The paper is organized as follows: first the action of VP on ice is described followed by results of full-scale indentation tests are formulated and then results on uniaxial compression tests are formulated. Finally, conclusions and discussions are given.

2. Action of vibrating plate on sea ice

The field works were performed on land fast ice in the Van Mijen Fjord near mining settlement Svea in March 2018 and 2019. In 2018, March 8-14, the ice thickness varied from 60 cm to 65 cm. The air temperature changed from -16 C to -22 C, and the mean ice temperature averaged over the ice thickness changed from -8.4 C to -11.35 C. The mean ice salinity was in the range of 5-7 ppt.

Figure 1. Vibrating plate on ice (left pane). Pulverization of ice surface by vibrating plate (right panel).
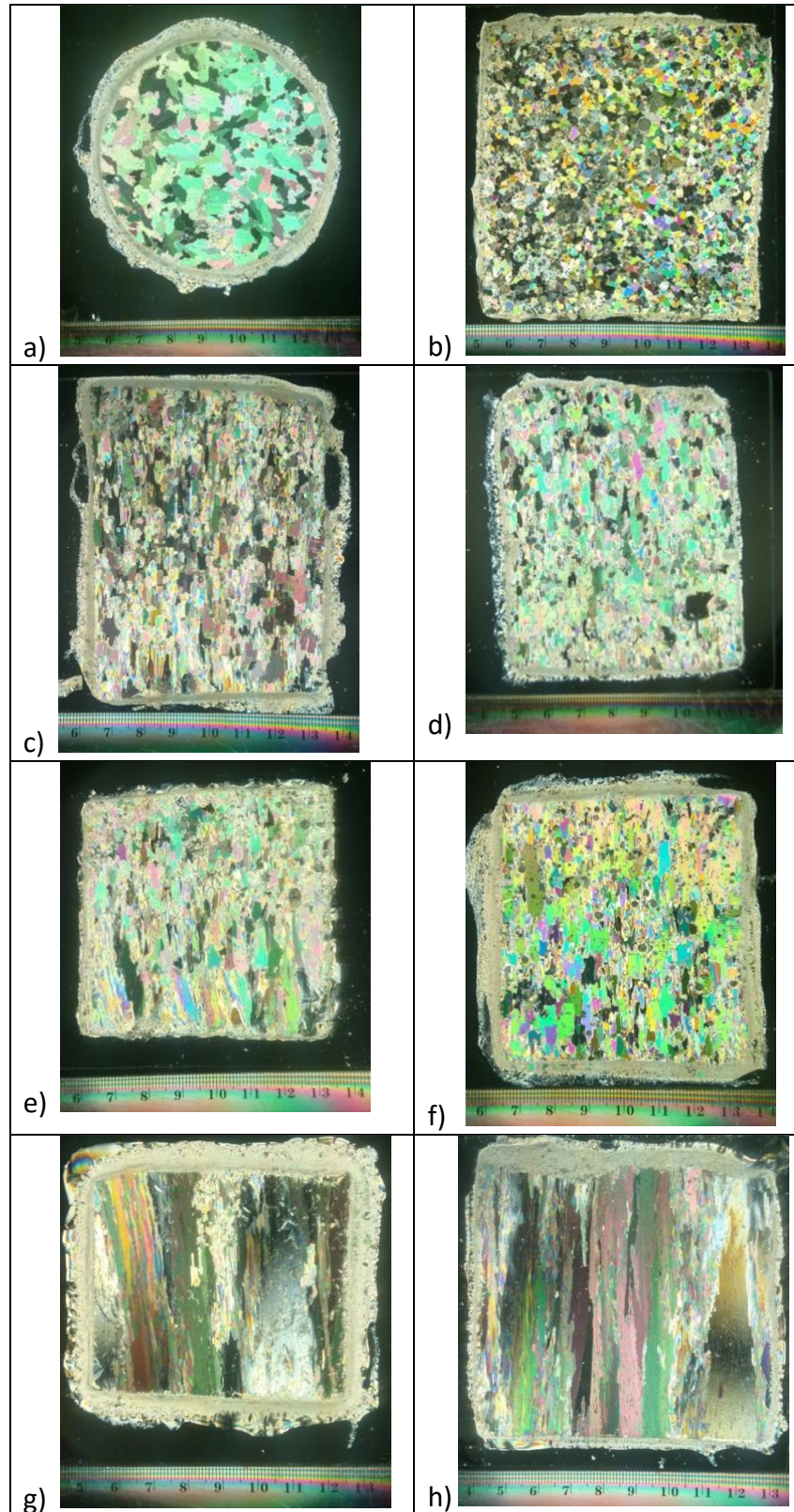
Figure 2. Horizontal sections of ice layer at 20 cm from the ice surface before (a) VP action, and at 5 cm from the ice surface after (b) VP action. Vertical sections of top layer of ice (10 cm from the surface) before (c) and after (d) VP action. Vertical sections of ice layer at 20 cm from the ice surface before (e) and after (f) VP action. Vertical sections of ice layer at 30 cm from the ice surface before (g) and after (h) VP action. March 2018.

Vibrating plate with weight of 400 kg was used during the field works (Fig. 1, left panel). VP can move forward or back and the intensity of vertical vibration of VP is regulated. Standing on a spot VP pulverizes ice below and gradually submerges into the ice (Fig. 1, right panel). Spectrum of accelerations of VP was measured with vibration recorder VibraCorder™ 4400A with the sampling frequency of 3.2 kHz. Maximum energy of vibrations was released at the frequency of about 80 Hz. VP was working on the ice during 10-15 min with maximal intensity of vibrations in each test, and then tests on the ice subjected by VP action were performed.

The ice cores taken from natural ice and from the ice subjected to the VP action, and thin sections were made from these ice cores with Microtom machine. Photos of thin sections in polarized light were made in Rigsby stage. All equipment for thin section analysis was installed in the tent on the place of the field works. Figure 2 shows the horizontal thin sections taken from the top layer of ice with thickness of 20 cm before (a) and after (b) of VP action on the ice. Since top layer of ice with thickness 8-10 cm was pulverized, we prepared thin section from the ice at 5 cm distance from the surface. Thus, both sections shown in Figs. 1a and 1b were prepared from the same ice. Fig. 2b shows very fine grain structure of ice immediately below VP. Figures 2c-h show vertical thin sections taken from the ice before (c, e, g) and after (d, f, h) VP action. The ice columns are destroyed up to 20 cm depth, and don't have significant changes at the depth of 30 cm below the ice surface.

3. Indentation tests

Full-scale indentation tests were performed with the original rig equipped with hydraulic cylinders A (upper cylinder) and B (lower cylinder) (Fig. 3). The capacity of each cylinder is 30 t. Each cylinder is equipped with stroke sensor and load cell. The principles of the functioning of the hydraulic system are described in (Marchenko et al, 2019). The indenter is vertical semi-circular cylinder of 15 cm diameter made from reinforced steel. Results of indentation tests were described in (Karulin et al., 2014; Marchenko et al., 2018). Lishman et al (2020) investigated acoustic emission in the indentation tests. The data of indentation tests includes records of strokes and loads on the cylinders A and B with sampling frequency 50 Hz.

Figure 3. Hydraulic rig for indentation tests.

It was visible during the indentation tests performed in March 2018 that the speed of indentation was higher in the tests performed in ice subjected to VP action. Figure 4 shows

interaction of the indenter with ice subjected to VP action (left panel) and with natural ice (right panel). The indenter practically didn't move in natural ice. Ice subjected to VP action failed by the formation of broken ice blocks or spoils on the surface. One can see in the left panel of Fig. 4 that top layer of ice with thickness of 7-8 cm is worn away due to VP action.

Figure 4. Indentation tests in the ice subjected to VP action (left panel) and in natural ice (right panel)
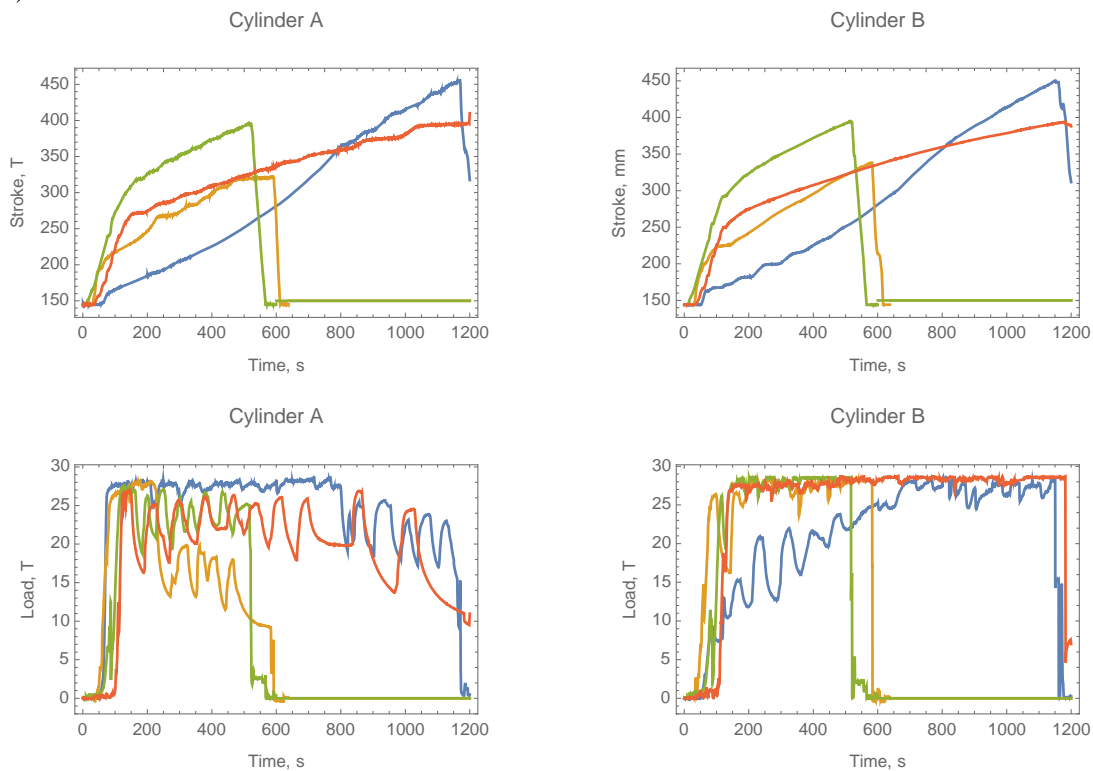

Figure 5. Records of strokes and loads in four indentation tests performed after VP action on natural ice. Blue, yellow, green and red colors correspond to the tests 1, 2, 3 and 4. March 2018.

Figure 5 shows records of strokes and loads on cylinders A and B recorded in four indentation tests performed after VP action on natural ice. The dependencies of strokes versus the time are similar for the cylinders A and B. Note that during the first 75 mm of penetration into the ice, the contact area of the circular-shaped indenter is increasing. This explains why the stroke speed is initially faster (tests 2, 3 and 4) and then slows down. The load on the cylinder A becomes smaller than the load on the cylinder B with the time because top layer of the ice was

damaged by VP action, and is thus 'softer'. The load oscillations on the cylinder A corresponds to events of ice break up in the surface layer similar to shown in Fig. 4 (left panel).
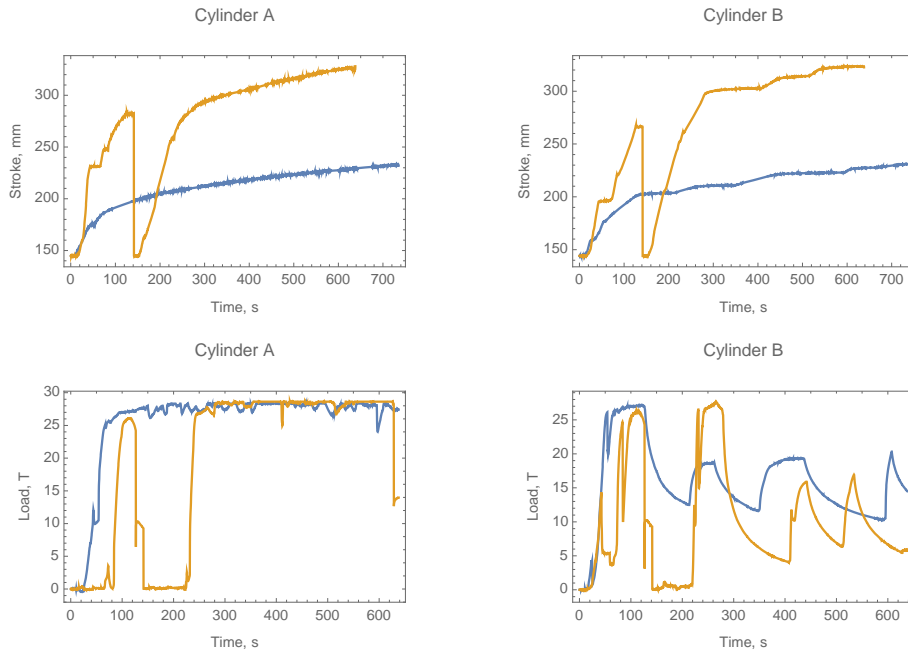

Figure 6. Records of strokes and loads in two indentation tests performed on natural ice. Blue and yellow lines correspond to the tests 5 and 6. March 2018.

Table 1. Mean stroke rates in the cylinders A (SRA) and B(SR) in Tests 1-6

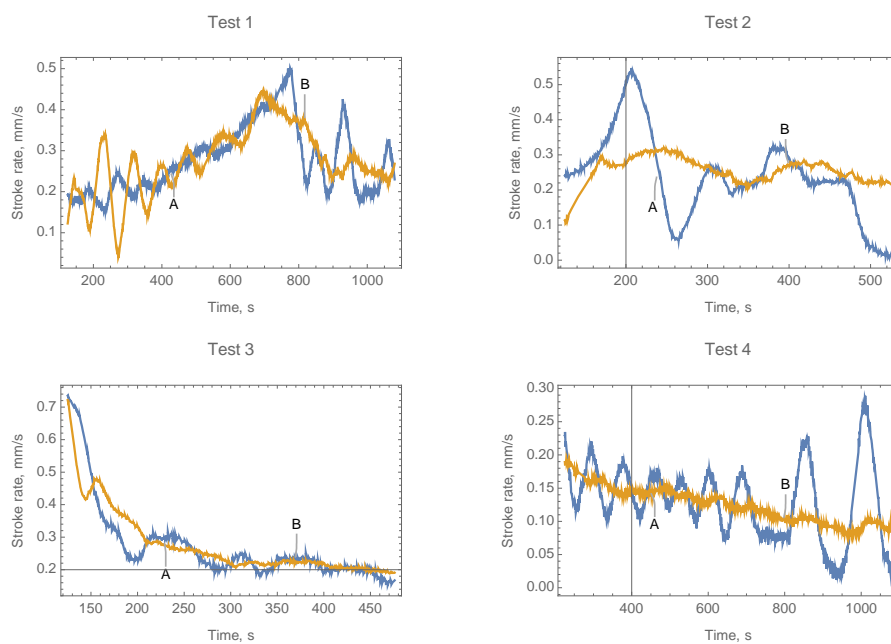| Test number	1	2	3	4	5	6
SRA, mm/s	0.277	0.240	0.271	0.132	0.076	0.102
SRB, mm/s	0.276	0.255	0.276	0.125	0.065	0.085

Figure 7. Stroke rates versus the time in four indentation tests performed after VP action on natural ice.

Figure 6 shows the records of strokes and loads in the indentation tests performed on natural ice. One can see that in contrast to Fig. 5 the load on the cylinder A is stable, and the load on cylinder B oscillates. It is explained by the failure of bottom layer of the ice which strength is smaller than the strength of surface ice layers because of the temperature effect.

Figure 7 shows the dependencies of stroke rates of the cylinders A and B in the tests 1-4 where ice was subjected to VP action, and Fig. 8 shows the dependencies of stroke rates of the cylinders A and B in the tests 5,6 in natural ice. Table 1 shows the mean values of the stroke rates averaged over the time intervals in Fig. 7 and Fig. 8. It is obvious that the stroke rates are greater in the tests 1-4 then in the tests 5, 6.
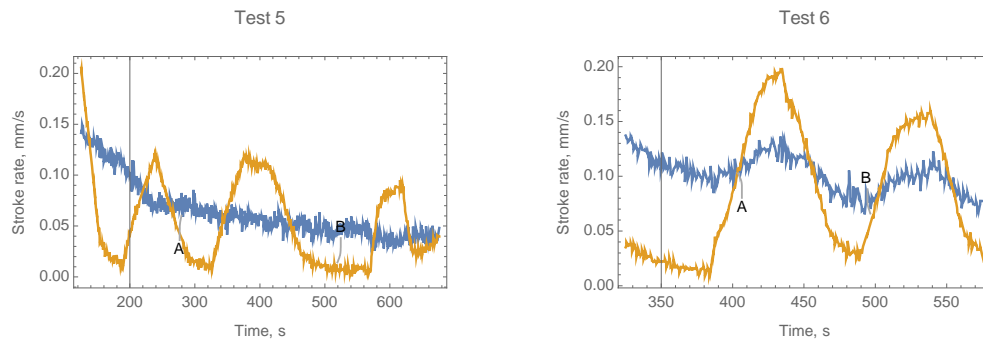

Figure 8. Stroke rates versus the time in two indentation tests performed on natural ice.

4. Uniaxial compression tests

Uniaxial compression tests were performed with vertical ice cores taken from the ice subjected to VP action on March 15 and from natural ice on March 10, 2019. All ice cores have the air temperature during the tests. The air temperature was -18C on March 10, and -14C on March 15. A representative temperature profile of ice cores is shown in Table 2. The salinity of ice cores varied within 5-7 ppt. The ice thickness was 70-75 cm. Tests were performed by the Kompis Rig (Moslet, 2007). Some of the tests were performed with cores (new cores) drilled soon after the ice was subjected by VP action. The other tests were performed with cores (old cores) drilled a few hours later after the ice was subjected by the action of the vibrating plate. Depth from which the new and old cores were taken was documented. We designate 'top layer' of ice extended from the ice surface to the depth of 20 cm, 'middle layer' of ice extended from the depth 20 cm to the depth 50 cm, and 'bottom layer' of ice located below 50 cm depth. Depth of the cores of natural ice was not written. All tests were performed at similar strain rate of $2 \cdot 10^{-4}$ s^{-1}. The length of all ice cores was 16 cm, and their diameter was 7.25 cm.

Table 2. Example of core temperature profile from March 10th

Depth (cm)	0	10	20	30	40	50	60
Temperature	-18.9	-18.3	-18.1	-17.7	-17.6	-17	-18

Figure 9 shows records of ice stress versus the time for all performed tests. One can see that most of the ice cores had brittle failure. Maximal stress in each test was interpreted as ice strength in uniaxial compression. Table 3 shows the ice strengths calculated from the tests

performed with ice cores taken from the ice subjected to VP action. Figure 10 shows the ice strengths of ice cores taken from natural ice. One can see that the strength of ice cores taken from the top layer of ice is smaller than the strength of ice cores taken from the middle and bottom layers. The mean strengths of the new and old cores are 10.8 MPa and 12.5 MPa. The mean strength of the ice samples from natural ice is 10.2 MPa.
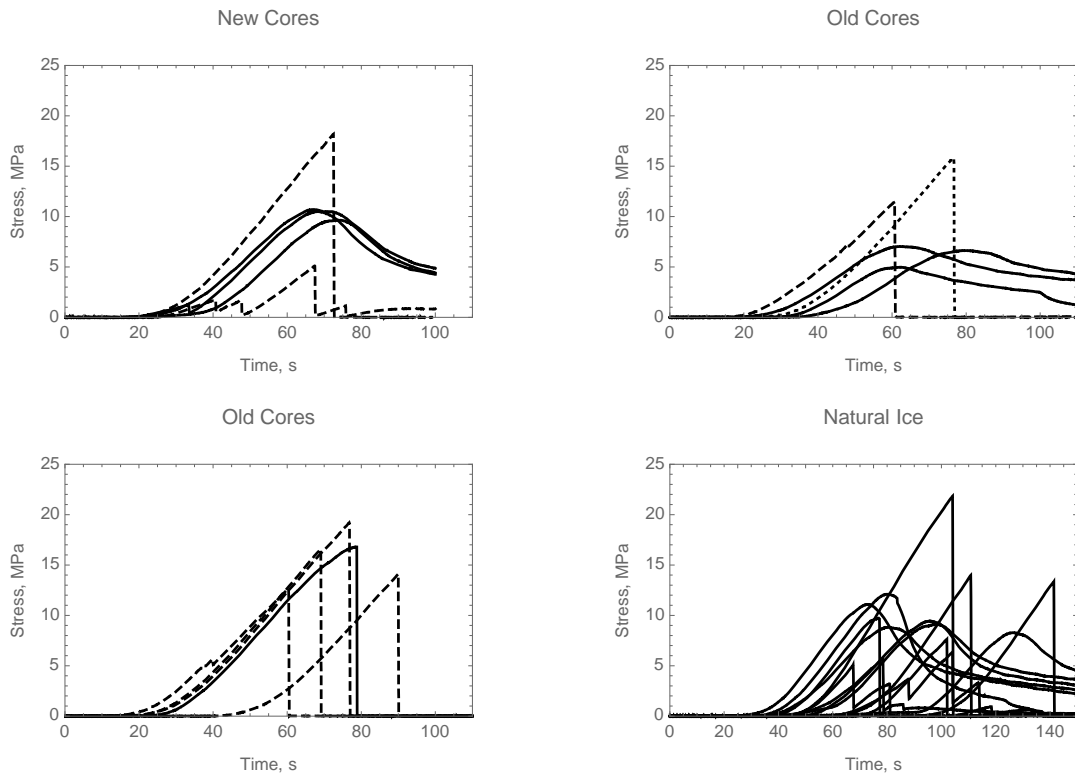

Figure 9. Stress versus the time in uniaxial compression tests with vertical ice cores. Solid, dashed and dotted lines correspond to the ice cores taken from 'top', 'middle' and 'bottom' layers of ice.
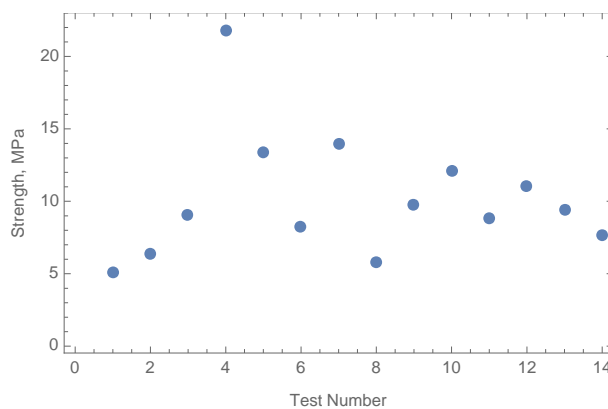

Figure 10. Ice strength after the uniaxial compression tests with vertical ice cores taken from natural ice.

The mean values and standard deviations of compression strength are shown in Table 4. We excluded the value 16.8 MPa (marked by gray color in Tab. 3) of the strength of old ice core taken from the top layer because this core demonstrated very different behavior from the other cores. Table 4 shows that the mean strength of old ice cores taken from the top layer of ice is

smaller the mean strength of new ice cores after vibrations. Standard deviation of the strength of ice cores after vibrations is lower than ice cores from natural ice.

Table 3. Uniaxial compression strength of new and old cores taken from 'top', 'middle' and 'bottom' layers of ice (MPa). D and B means ductile and brittle failure.

New	Top	9.63, D	10.69, D	10.5, D		
	Middle	18.19, B	5.1, B			
Old	Top	6.62, D	7.03, D	4.97, D	16.8, B	
	Middle	11.47, B	19.21, B	14.12, B	12.66, B	16.59, B
	Bottom	15.85, B				

Table 4. Uniaxial The mean values and standard deviation of compression strength.

	New, Top	Old, Top	Old, Middle	Natural ice
Mean	10.27	6.2	14.81	10.18
St. Dev.	0.56	1.09	3.11	4.29

We assume that VP influenced the top ice layer stronger than the middle and the bottom layers. Experiments showed higher strength in the middle (14.81 MPa) and bottom (15.85 MPa) layers than in the top layer (10.27 MPa) of ice subjected to VP action. The averaged strength of natural ice (10.18 MPa) was almost the same as in the top layer ice (10.27 MPa). If the strength of top layer natural ice would be 6.2 MPa, and the strengths of middle and bottom layers of natural ice would be respectively 14.81 MPa and 15.85 MPa then the mean strength of natural ice would be 12.29 MPa. It indicates strengthening of the top ice layer immediately after the VP action and decreasing of the ice strength in the top layer after several hours.

5. Discussion and Conclusions

The influence of cyclic deformation on ice properties was discussed in several papers. Usually cyclic deformations of materials lead to fatigue failure after certain number of cycles. Haynes et al (1993) investigated the influence of pulsating load on bearing capacity of floating fresh ice. The pulsation frequencies of 21.5 Hz and 15 Hz were applied in the experiments. After ice failure was not observed in the experiments, they were turned to investigate the influence of pulsating load on bearing capacity of ice. Test results showed lowering the bearing capacity due to the oscillations. Haskell et al (1996) performed in-situ tests on cyclic deformations of floating cantilever beams made of sea ice in the Antarctic. The periods of bending deformations were ~10 s. The dependence of bending stress at the beam failure from the number of cycles was investigated. It was discovered that ice doesn't fail if maximal stress is lower a half of the flexural strength.

In contrast to above mentioned effect of ice weakening under cyclic loading the ice strengthening was also discovered mainly for laboratory made ice. The ice strengthening due to uniaxial cyclic deformations tension-compression was described by Cole (1990). The experiments were performed in the frequency range of 0.001-10 Hz. Limited observations indicated an increase of brittle tensile strength of specimens after cycling loading. Increase of the flexural strength of laboratory made ice beams after their cyclic bending was discussed in the papers (Iliescu et al, 2017; Murdza et al, 2020a). Most of the bending cycles were performed with period of 10 s. It was discovered that flexural strength may increase even when the stress amplitude during cycling exceeds a half of flexural strength of not cycled samples. Similar

experiments on cyclic 3-ponts bending of beams made from fresh-water lake ice also demonstrated small strengthening in comparison with tests with laboratory made ice beams (Murdza et al, 2020b).

In the present paper we investigated the influence of vibrations with higher frequency (80 Hz) on the strength of natural columnar sea ice. Vibrations were introduced in the ice in parallel direction to ice columns by vibrating plate working on the ice during 15 min. Vibrating plate pulverized surface layer of ice with thickness smaller 10 cm and caused strongest influence on the property of ice layer below the pulverized ice. Two types of in-situ tests were performed: full scale indentation tests on floating ice and uniaxial compression tests with ice cores. The indentation tests showed weakening of ice in the horizontal directions after the action of vibrating plate. The uniaxial compression tests indicated an increase of ice strength in the vertical direction in the top layer immediately after the action of vibrating plate on ice, and further reduction of this strength with the time.

Obtained results demonstrate the influence of the direction of applied vibrations on the strengthening of columnar sea ice. In combination with results from (Haynes et al, 1993) it is possible to conclude that vertical vibrations increase compression strength in the vertical direction and reduce ice strength in the horizontal directions. For the further studies we plan to perform more uniaxial compression tests with vertical and horizontal ice cores taken from natural ice and ice subjected to the action of vibrating plate. It is of interest to investigate the influence of vibrations applied in perpendicular directions to ice columns.

References

Bogorodsky, V.V., Gavrilo, V.P., Nedoshivin, O.A., 1987. Ice destruction. Methods and Technology. D.Reidel Publishing Company, Dordrecht, Holland.

Cole, D.M., 1990. Reversed direct-stress testing of ice: Initial experimental results and analysis. Cold Regions Science and Technology, 18, 303–321.

Haynes, F.D., Kerr, A.D., Martinson, C.R., 1993. Effect of fatigue on the bearing capacity of floating ice sheets. Cold Regions Science and Technology, 21, 257–263.

Haskell, T.G., Robinson, W.H., Langhorne, P.J., 1996. Preliminary results from fatigue tests on in situ sea ice beams. Cold Regions Science and Technology, 24, 167–176.

Iliescu, D., Murdza, A., Schulson, E.M., Renshaw, C.E., 2017. Strengthening ice through cyclic loading. J. Glaciology, 63 (240), 663-669.

Karulin, E., Marchenko, A., Karulina, M., Chistyakov, P., Sakharov, A., Ervik, A., Sodhi, D., 2014. Field Indentation Tests of Vertical Semi-Cylinder on First-Year Ice. Proc. of the 22th IAHR Symposium on Ice, Singapore, paper 1125.

Lezin, D.L., 1977. Icebreaker attachements. Proc. of Research Institute of Water Transport, 126, 3-15. (in Russian).

Lishman, B., Marchenko, A., Sammonds, P., Murdza, A., 2020. Acoustic emissions from in situ compression and indentation experiments on sea ice. Cold Regions Science and Technology, 172, 102987.

Marchenko, A., Karulin, E., Karulina, M., Sakharov, A., Chistyakov, P., Sodhi, D., Sliusarenko, A., 2018. Scale effects in compressive strength of sea ice. Proc. of the 24th IAHR Symposium on Ice, Vladivostok, paper 18-004.

Marchenko, A., Karulin, E., Sakharov, A., Chistyakov, P., 2019. On the influence of the hydraulic   characteristics of the rig during full-scale compression and indentation tests on sea ice. POAC-32.

Moslet, P.O., 2007. Field testing of uniaxial compression strength of columnar sea ice. Cold Regions Science and Technology, 48 (1), 1–14.

Murdza, A., Schulson, E.M., Renshaw, C.E., 2020a. Strengthening ice through cyclic loading. J. Glaciology, 1-11.

Murdza, A., Marchenko, A., Schulson, E.M., Renshaw, C.E., 2020b. Cyclic strengthening of lake ice. J. Glaciology, 1-11. (accepted)